Boronic Acid Shell-Crosslinked Dextran-*b*-PLA Micelles for Acid-Responsive Drug Delivery[a]

Ziwei Zhao, Xuemei Yao, Zhe Zhang, Li Chen,* Chaoliang He, Xuesi Chen

Herein, 3-carboxy-5-nitrophenylboronic acid (CNPBA) shell-crosslinked micelles based on amphiphilic dextran-*block*-polylactide (Dex-*b*-PLA) are prepared and used for efficient intracellular drug deliveries. Due to the reversible pH-dependent binding with diols to form boronate esters, CNPBA modified Dex-*b*-PLA shows excellent pH-sensitivity. In neutral aqueous conditions, CNPBA-Dex-*b*-PLA forms shell-crosslinked micelles to enable DOX loading, while in acid conditions, the boronate esters hydrolyze and the micelles de-crosslink to release loaded DOX. In vitro release studies indicate that the release of the DOX cargo is minimized at physiological conditions, while there is a burst release in response to low pHs. The cell viability of CNPBA-Dex-*b*-PLA investigated by MTT assay was more than 90%, indicating that, as a drug delivery system, CNPBA-Dex-*b*-PLA has good cytocompatibility. These features suggest that the pH-responsive biodegradable CNPBA-Dex-*b*-PLA can efficiently load and deliver DOX into tumor cells and enhance the inhibition of cellular proliferation in vitro, providing a favorable platform as a drug delivery system for cancer therapy.

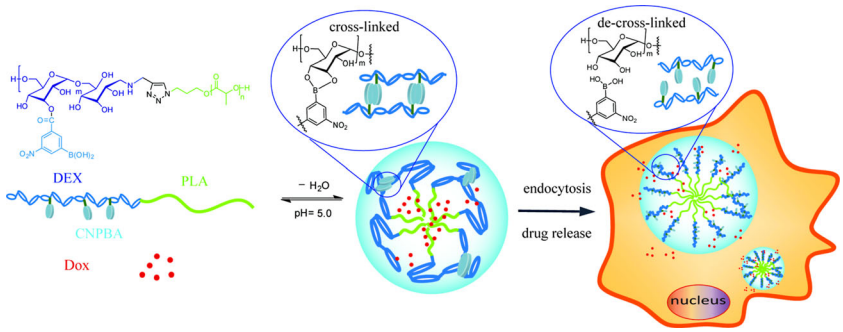

1. Introduction

Over the past few decades, nanocarriers have emerged as one of the most fascinating delivery vehicles for small molecular antitumor drugs, such as doxorubicin (DOX),[1–4] paclitaxel (PTX),[5] and docetaxel,[6] to improve therapeutic efficiency and eliminate adverse effects on organisms due to their accumulation in tumors via the passive "enhanced permeability and retention (EPR) effect". Among these nanocarriers, stimuli-responsive nanoparticles offer the opportunity to selectively deliver a drug on demand to a specific location within the human body. External or physiological stimuli, such as pH,[7–9] temperature,[10–11] light[12–13], reductive,[13–15] or enzymes,[16] have attracted tremendous attention as triggers for intelligent carriers to release drugs. These stimuli responsive carriers are noted for their site-specific targeted release of payloads modulated by the specific microenvironments of the intracellular space, leading to aggressive anticancer activity and maximal chemotherapeutic efficacy with fewer side effects.[17]

Compared with the neutral pH environment in most human tissues, mildly acidic conditions may be found in sites of inflammation, lysosomal compartments, or tumor

Z. Zhao, X. Yao, Z. Zhang, L. Chen
Department of Chemistry, Northeast Normal University, Changchun 130024, P. R. China
E-mail: chenl686@nenu.edu.cn
C. He, X. Chen
Changchun Institute of Applied Chemistry, Chinese Academy of Sciences, Changchun 130022, P. R. China

[a]**Supporting Information** is available at Wiley Online Library or from the author.

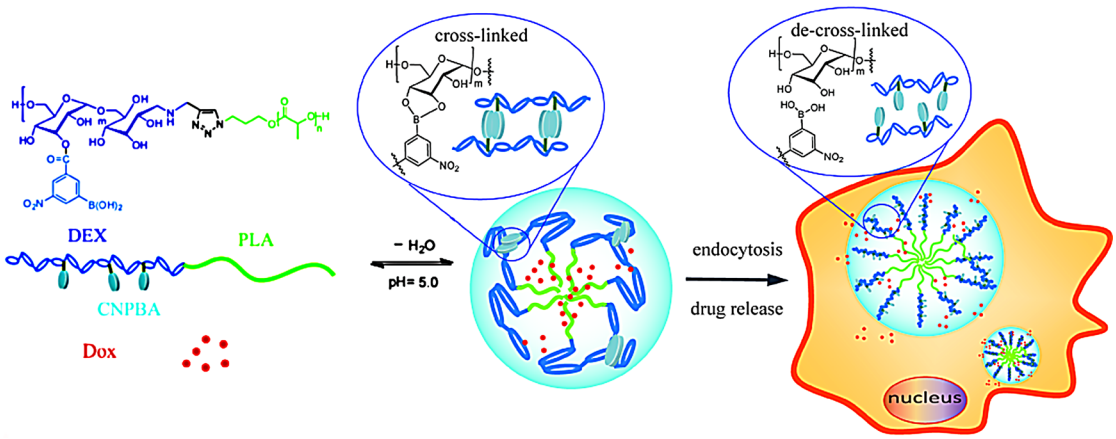

Scheme 1. Schematic illustration of DOX loading and release from DOX-loaded PDP-m.

tissue. Because of this change in the physiological environment, choosing pH as an internal stimulus has become the most common method used to prepare smart responsive drug delivery systems. Compared with the conventional specific tumor cell surface targeting approach, this pH-targeting approach is considered to be a more general strategy because of the acidic tumor microclimate in solid tumors. Hence, many acid-labile chemical bonds, such as maleic acid amide,[18] acetal,[19] hydrazone,[20] and orthoester,[21] have been extensively employed to design acid-responsive drug delivery systems.

It is well known that boronic acids can reversibly bind with diols to form boronate esters, one of the key precursors of boronic acid derivatives, which exhibit fast responsiveness to both the external pH environment and competing diols.[22–24] Under acidic conditions, boronic esters exhibit pH-responsiveness and can be easily hydrolyzed. As a kind of boronic acid, phenylboronic acid (PBA) and its derivatives can specifically interacted with mannitol and other polyols to form phenylboronates. There are two forms of PBA moieties at equilibrium in water: (1) the neutral and hydrophobic form with the triangular plane structure ($pH < pK_a$ of PBA); (2) the charged and hydrophilic form where PBA groups have a tetrahedral structure ($pH > pK_a$ of PBA).[25] Based on these two forms, phenylboronates show an excellent pH-sensitive property. On the other hand, the formation of boronate esters can further improve the hydrophilicity of PBA-functionalized polymers, resulting in the swelling of the matrix and the release of payloads. Taking advantage of this reversible change, PBA has been chosen as a promising candidate for nanocarriers and has been immobilized in various matrices.[26–32] Zhang et al. have reported the formation of pH-responsive polymer nanoparticles by crosslinking dextran with poly(3-acrylamidophenylboronic acid).[33] Li has modified dextran with hydrophobic phenylboronic ester functionalities to spontaneously form acid-responsive nanoparticles in water.[34] Therefore, boronic ester-containing polymers with unique reactivity and self-assembly capability have significant potential applications as sensors for sugars and glycoproteins, and in self-regulated drug delivery systems and therapeutic agents.

Polymeric micelles based on amphiphilic copolymers, as one kind of antitumor drug nanocarrier, have received considerable attention due to their greatly enhanced water solubility and their prolonged circulation in blood. However, one practical challenge with their application is their low stability in vivo. In order to overcome this limitation, different shell or core crosslinking approaches have been adopted, which can not only improve the stability of micelles, but also control drug release through environment responsive linkages. Herein, 3-carboxy-5-nitrophenylboronic acid (CNPBA) was chosen as a crosslinker to prepare shell-crosslinked micelles based on Dex-*b*-PLA copolymers. Dex-*b*-PLA copolymers were first prepared by a click reaction and were then modified by the crosslinker CNPBA to obtain CNPBA-Dex-*b*-PLA. Taking advantage of its pH-sensitivity, DOX, as a model anticancer drug, was loaded into the shell-crosslinked micelles, as shown in Scheme 1. This type of pH-sensitive micelle could rapidly respond to the acidic intracellular compartments of carcinoma cells, and therefore holds great potential for in vivo chemotherapeutics.

2. Experimental Section

2.1. Materials

$_{L}$-Lactide ($_{L}$-LA, Purac) and $_{D}$-lactide ($_{D}$-LA, Purac) were recrystallized three times from ethyl acetate under an argon atmosphere. Dextran (Dex, $\overline{M}_n = 6$ kDa, Sigma), 3-bromo-1-propanol (Sigma), sodium

azide (Sigma), stannous octoate (tin (II)-bis (2-ethylhexanoate) ($Sn(Oct)_2$, 95% Sigma), propargylamine (98% Sigma), sodium cyanoborohydride (Sigma), N,N,N′,N′,N″-pentamethyldiethylenetriamine (PMDETA, Sigma), 3-carboxy-5-nitrophenylboronic acid (Sigma), 1-(3-dimethylaminopropyl)-3-ethylcarbodiimide (EDC) (Sigma), 4-dimethylaminopyridine (DMAP) (Sigma), and copper bromide (Sigma) were used as received. Toluene was dried by refluxing over Na metal under an argon atmosphere and distilled immediately before use. Dimethyl sulfoxide (DMSO) was dried over calcium hydride (CaH_2) and purified by vacuum distillation with CaH_2. Acetate buffer with a concentration of 0.2 mol L^{-1} was prepared by mixing acetic acid and sodium acetate at pH 5.0. Dry 3-(4,5-dimethyl-thiazol-2-yl)-2,5-diphenyl tetrazolium bromide (MTT) was purchased from Sigma-Aldrich. Doxorubicin hydrochloride (DOX · HCl) was purchased from Zhejiang Hisun Pharmaceutical Co., Ltd.

2.2. Characterization

^{1}H NMR spectra were recorded on a Bruker AV 400 NMR spectrometer in dimethyl sulfoxide-d_6 (DMSO-d_6) or chloroform-d_1 ($CDCl_3$-d_1). Fourier Transform infrared (FTIR) measurements were recorded on a Bio-Rad Win-IR instrument using the potassium bromide (KBr) method. Gel permeation chromatography (GPC) analyses were performed on a Polymer Laboratories PL-GPC 50 Plus integrated GPC system with two Jordi DVB mixed bed columns (300 × 7.5 mm) and absolute molecular weights were obtained using a refractive index detector coupled to a multiangle laser light scattering detector, the MiniDAWN Treos (Wyatt Technology, USA). GPC analyses were carried out in HPLC-grade $CHCl_3$ (flow rate: 1 mL min^{-1}) at 50 °C on samples of 1 mg mL^{-1} concentration. Dynamic light scattering (DLS) measurements were performed on a WyattQELS instrument with a vertically polarized He-Ne laser (DAWN EOS, Wyatt Technology) and 90° collecting optics. All the samples were prepared in aqueous solution at a concentration of 0.25 mg mL^{-1}. Transmission electron microscopy (TEM) measurements were performed using a JEOL JEM-1011 transmission electron microscope with an accelerating voltage of 100 kV. A drop of the sample solution (0.25 mg mL^{-1}) was deposited onto a 230 mesh copper grid coated with carbon and allowed to dry in air at 25 °C before measurement.

2.3. Synthesis of α-Azido PLA (N_3-PLA)

The introduction of the azide group to the PLA backbone was conducted in two steps described in Scheme 2a. First, sodium azide (0.3 g, 4.62×10^{-3} mol) was dissolved in 20.0 mL of 3-bromo-1-propanol in a flame-dried flask and the reaction was maintained at room temperature for 48 h. Second, an equimolar mixture of $_L$-lactide and $_D$-lactide (10.0 g, 69.4×10^{-3} mol) was dissolved in 30.0 mL of anhydrous toluene in a flame-dried flask at room temperature. Then, α-azido propanol (0.19 mL, 2.5×10^{-3} mol) and $Sn(Oct)_2$ (28.12 mg, 69.4×10^{-6} mol, 0.001 equiv.) were added into the solution with stirring and the ROP reaction was maintained at 85 °C for 4 d. After precipitating the solution into excessive diethyl ether, the crude product was further washed twice with diethyl ether and dried under a vacuum at room temperature for 24 h to obtain the resultant N_3-PLA (8.0 g; yield: 80%). The molecular weight of N_3-PLA was calculated from ^{1}H NMR and GPC measurements.

2.4. Synthesis of α-Alkyne Dextran (Alkyne-Dex)

The modification of dextran was conducted as shown in Scheme 2b. Typically, dextran (4.0 g, 0.66×10^{-3} mol) was dissolved in 2% (w/v) acetate buffer (pH 5.0) in a flask at 50 °C. Propargylamine (0.684 g, 9.8×10^{-3} mol, 15 equiv.) and sodium cyanoborohydride (0.628 g, 9.9×10^{-3} mol, 15 equiv.) were added under stiring. The mixture was allowed to stir at 50 °C for 96 h. The solution was then concentrated using a rotavapor, and dialyzed against deionized water (MWCO 3.5 kDa) for 2 d. The product was collected by lyophilization (2.8 g; yield: 70%).

2.5. Synthesis of Dextran-*block*-Polylactide (Dex-*b*-PLA)

Dex-*b*-PLA was synthesized by Huisgen's 1,3-dipolar cycloaddition ("click chemistry") shown in Scheme 2c. A typical procedure for the preparation is briefly described as follows. N_3-PLA (0.2 g, 0.06×10^{-3} mol), alkyne-Dex (0.6 g, 0.1×10^{-3} mol) and PMDETA (21 μL, 0.1×10^{-3} mol) were dissolved in 30.0 mL of dried DMSO with stirring for 30 min. After being degassed by three freeze-thaw cycles, the mixture was transferred into another Schlenk flask containing CuBr (14.4 mg, 0.1×10^{-3} mol) via a N_2-purged syringe in an oil bath at 60 °C for 72 h. After the reaction finished, the reaction medium was dialyzed against deionized water (MWCO 7 kDa) for 4 d and the product was obtained by lyophilization (0.5 g; yield: 63%).

2.6. Synthesis of CNPBA Modified Dex-*b*-PLA (CNPBA-Dex-*b*-PLA)

The mechanism is based on the condensation reaction, as shown in Scheme 2d. Typically, Dex-*b*-PLA (1.0 g, 0.11×10^{-3} mol), CNPBA (0.17 g, 0.82×10^{-3} mol), EDC (0.31 g, 1.64×10^{-3} mol, 2 equiv.), and DMAP (0.02 g, 0.16×10^{-3} mol, 2 equiv.) were dissolved in 15.0 mL of DMSO with stirring for 24 h at room temperature. After the reaction finished, the reaction medium was dialyzed against deionized water (MWCO 7 kDa) for 4 d and the product was obtained by lyophilization (0.81 g; yield: 69%).

2.7. In Vitro Drug Loading and Release

Doxorubicin (DOX) was chosen as a model drug for in vitro drug loading and release. DOX-loaded micelles were prepared by a simple dialysis technique. Typically, PDP-m (15 mg), DOX · HCl (3.0 mg), and triethylamine (0.9 mg) were mixed in 2.0 mL of DMSO. The mixture was stirred at room temperature for 24 h and then added dropwise into 20.0 mL of PBS at pH 7.4. The DMSO was removed by dialysis against deionized water for 24 h. The dialysis medium was refreshed five times and the whole procedure was performed in the dark. Then, the solution was filtered and lyophilized. To determine the drug loading content (DLC) and drug loading efficiency (DLE), the drug-loaded micelles were dissolved in DMSO and analyzed by fluorescence measurements (Perkin-Elmer

Macromol. Biosci. **2014,** DOI: 10.1002/mabi.201400251

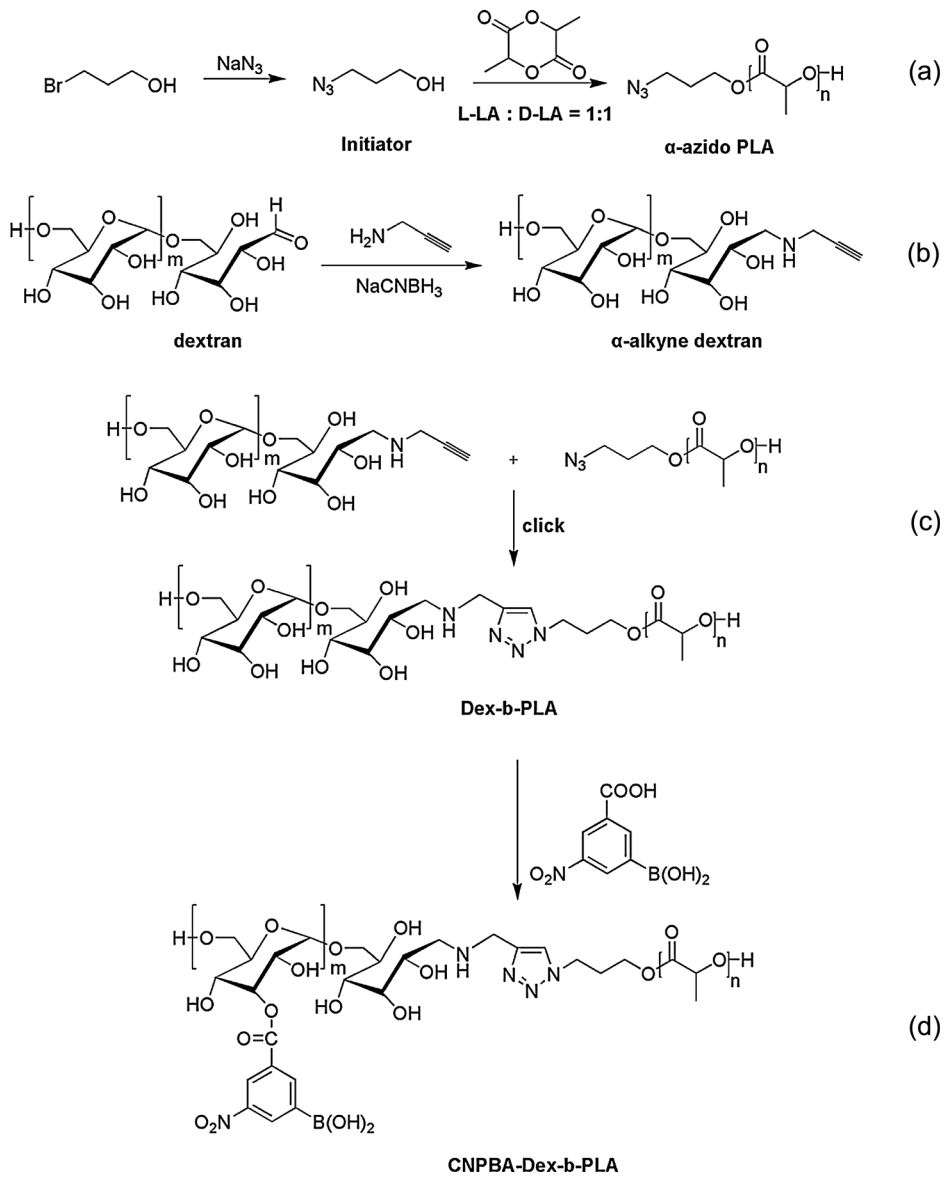

Scheme 2. Synthetic routes to CNPBA-Dex-*b*-PLA.

LS50B luminescence spectrometer) using a standard curve method ($\lambda_{ex} = 480$ nm). The DLC and DLE of DOX-loaded micelles were calculated according to Equation (1) and Equation (2), respectively:

$$DLC(wt\%) = \frac{amount\ of\ drug\ in\ micelles}{amount\ of\ drug\ loaded\ micelles} \times 100 \quad (1)$$

$$DLE(wt\%) = \frac{amount\ of\ drug\ in\ micelles}{total\ amount\ of\ feeding\ drug} \times 100 \quad (2)$$

In vitro drug release profiles of DOX-loaded micelles were investigated in PBS at pH 5.5, 6.8, and 7.4, respectively. The weighed freeze-dried DOX-loaded micelles were suspended in 10.0 mL of release medium and transferred into a dialysis bag (MWCO 3.5 kDa). The release experiment was initiated by placing the end-sealed dialysis bag into 50 mL of PBS at 37 °C with continuous shaking at 100 rpm. At pre-determined time intervals, 2.0 mL of dialysate was taken out and an equal volume of fresh PBS was replenished. The amount of released DOX was determined by fluorescence measurements ($\lambda_{ex} = 480$ nm). The release experiments were conducted in triplicate.

2.8. Intracellular Drug Release

The cellular uptake and intracellular release behaviors of DOX-loaded micelles were assessed by confocal laser scanning microscopy (CLSM) and flow cytometry on MCF-7 cells.

Macromolecular Journals

Macromol. Biosci. **2014,** DOI: 10.1002/mabi.201400251

2.8.1. Confocal Laser Scanning Microscopy (CLSM)

For CLSM studies, MCF-7 cells were seeded in 6-well plates at a density of 1×10^5 cells per well in 2.0 mL of complete Dulbecco's modified Eagle's medium (DMEM) containing 10% fetal bovine serum, supplemented with 50 IU mL^{-1} penicillin and 50 IU mL^{-1} streptomycin, and cultured for 24 h. After the culture media were removed, the cells were incubated at 37 °C for an additional 3 h with DOX-loaded micelles at a final DOX concentration of 10.0 mg L^{-1} in complete DMEM. Then, the culture medium was removed and cells were washed with PBS three times. Thereafter, the cells were fixed with 4% paraformaldehyde for 30 min at room temperature, and the cell nuclei were stained with 4′,6-diamidino-2-phenylindole (DAPI, blue) for 20 min. CLSM images of cells were obtained through a confocal microscope (Olympus FluoView 1000).

2.8.2. Flow Cytometric Analysis

MCF-7 cells were seeded in 6-well plates at 1×10^5 cells per well in 2.0 mL of complete DMEM and cultured for 24 h. The cells were then washed with PBS and incubated at 37 °C for an additional 3 h with DOX-loaded micelles at a final DOX concentration of 10.0 mg L^{-1} in complete DMEM. Thereafter, the culture medium was removed and the cells were washed with PBS three times and treated with trypsin. Then, 1.0 mL of PBS was added to each culture well, and the solutions were centrifuged for 5 min at 1000 rpm. After the removal of supernatants, the cells were resuspended in 0.2 mL of PBS. Data for 1×10^4 gated events were collected, and analysis was performed by flow cytometry (Beckman, California, USA).

2.9. Cell Viability Assays

The relative cytotoxicities of micelles against HeLa cells and MCF-7 cells were evaluated in vitro using a standard MTT assay. The cells were seeded in 96-well plates at 7000 cells per well in 200.0 μL of complete DMEM and incubated at 37 °C in a 5% CO_2 atmosphere for 24 h. The culture medium was then removed and micelle solutions in complete DMEM at different concentrations (0–10 g L^{-1}) were added. The cells were subjected to the MTT assay after being incubated for an additional 72 h. The absorbance of the solution was measured on a Bio-Rad 680 microplate reader at 490 nm. Cell viability (%) was calculated based on Equation (3):

$$Cell\ viability(\%) = \frac{A_{sample}}{A_{control}} \times 100 \quad (3)$$

where, A_{sample} and $A_{control}$ represent the absorbance of the sample and control wells, respectively.

The cytotoxicities of DOX-loaded micelles against HeLa cells and MCF-7 cells were also evaluated in vitro by a MTT assay. Similarly, cells were seeded into 96-well plates at 7000 cells per well in 200.0 μL of complete DMEM and incubated for 24 h. After washing cells with PBS, 180.0 μL of complete DMEM and 20.0 μL of DOX-loaded micelle solutions in PBS were added to form culture media with different DOX concentrations (0–10.0 mg L^{-1} DOX). The cells were subjected to the MTT assay after being incubated for 24, 48, and 72 h. The absorbance of the solution was measured on a Bio-Rad 680 microplate reader at 490 nm. Cell viability (%) was also calculated based on Equation (3).

3. Results and Discussion

3.1. Synthesis of CNPBA-Dex-*b*-PLA

Dex-*b*-PLA was synthesized by combining the clickable alkyne-Dex with N_3-PLA precursor via click chemistry, as depicted in Scheme 2. Firstly, atactic-PLA was synthesized via the ring-opening polymerization of an equimolar mixture of $_L$-lactide and $_D$-lactide by varying the ratio of lactide to α-azido propanol. The ^{1}H NMR spectrum of N_3-PLA in $CDCl_3$ is shown in Figure S1 in the Supporting Information. The peaks at 5.15–5.25 ppm and 1.5 ppm were attributed to the characteristic signals of the PLA units. According to the ^{1}H NMR spectrum,[35] the molecular weight of atactic-PLA was 3000 in accordance with that obtained from gel permeation chromatography (GPC). From GPC, the molecular weight of atactic-PLA was 3346 with a PDI of 1.84. In order to conduct the click reaction, an alkyne group was introduced into dextran by reductive amination with propargylamine in acetate buffer solution (pH 5.0). The chemical structure of alkyne-Dex was confirmed by ^{1}H NMR. As shown in Figure S2 in the Supporting Information, the complete disappearance of the anomeric proton peaks at 6.7 and 6.3 ppm belonging to the reducing end group quantitatively indicated the successfully synthesis of α-alkyne dextran. Then the amphiphilic Dex-*b*-LA was synthesized by a click reaction. As shown in Figure 1, the methine protons peaks at 5.15–5.25 ppm were attributed to the characteristic signals in PLA units and the peaks at 3–4 ppm were assigned to the protons of the dextran. This further indicated the successful synthesis of amphiphilic Dex-*b*-PLA copolymers.

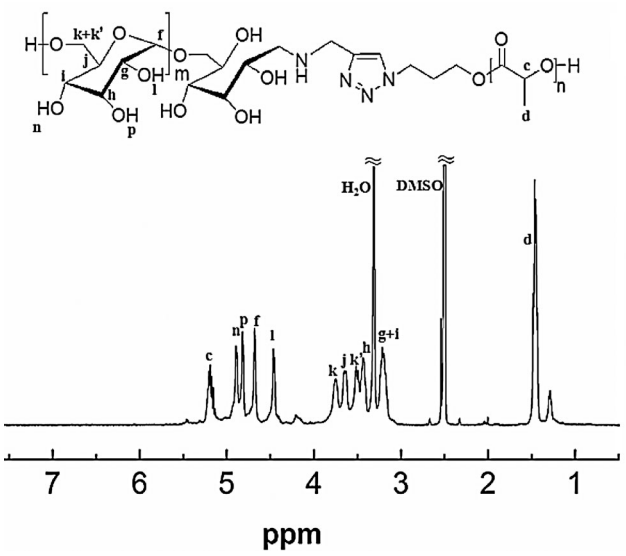

Figure 1. ^{1}H NMR spectrum of Dex-*b*-PLA in DMSO-d_6.

Table 1. Characterization of PDP-m.

Sample	Entry	Ratio[a)] [%]	Ratio[b)] [%]	CMC[c)] [mg mL^{-1}]	DLS[c)] [nm]	DLC [wt%]	DLE [wt%]
Dex-*b*-PLA	PDP-0	–	–	0.033	59.9 ± 6.2	8.7	51.2
$CNPBA_1$-Dex-*b*-PLA	PDP-1	5	3.7	0.033	56.4 ± 5.7	9.0	53.7
$CNPBA_2$-Dex-*b*-PLA	PDP-2	10	9.5	0.027	44.2 ± 5.3	9.3	56.7
$CNPBA_3$-Dex-*b*-PLA	PDP-3	20	17.3	0.021	31.1 ± 4.8	10.2	61.3

[a)]Theoretical grafting ratio of CNPBA, refered to as the ratio of CNPBA to glucose residue; [b)]Actual grafting ratio of CNPBA by UV-vis; [c)]Determined in PBS at 7.4.

CNPBA-Dex-*b*-PLAs were prepared by a condensation reaction via the hydroxyl group of Dex-*b*-PLA and the carboxyl group of CNPBA. FT-IR spectra are shown in Figure S3 in the Supporting Information. The peak at 1530 cm^{-1} belonging to the phenyl group suggested the successful modification of Dex-*b*-PLA by CNPBA. The grafting ratios of CNPBA were calculated by a UV-vis method, as show in Figure S4 in the Supporting Information. According to the standard curve, the actual grafting ratio of CNPBA in PDP-m was obtained, as listed in Table 1.

3.2. Characterization of Shell-Crosslinked Polymer Micelles

It is known that boronic acid can easily react with hydroxyl groups to form boronate ester in neutral aqueous solution. There are abundant functional hydroxyl groups along the chain of dextran, so CNPBA-Dex-*b*-PLA can self-assemble to form shell-crosslinked micelles in neutral aqueous conditions. The self-assembly of CNPBA-Dex-*b*-PLA was characterized by fluorescence spectra using Nile Red as the fluorescence probe, according to a literature method.[36–37] The critical micelle concentration (CMC) could be calculated by tracking the fluorescence intensity of Nile Red as a function of the sample concentration, as shown in Figure S5 in the Supporting Information and Table 1. At pH 7.4, PDP-3 showed a lower CMC value of 0.021 mg mL^{-1} than that of PDP-0 (0.033 mg mL^{-1}) because boronic acid from CNPBA reacted with the hydroxyl group of dextran to form shell-crosslinked micelles at lower concentrations. The CMC values of PDP-0 and PDP-1 were very similar due to the actual grafting ratio of CNPBA for PDP-1 being only 3.7%.

As is well known, crosslinked boronate ester bonds undergo hydrolysis in acidic conditions, which would result in the de-crosslinking of the crosslinked micelles. This pH-sensitivity was further verified by the change of CMC value with pH value. For PDP-0 micelles, the CMC values were the same at both pH 5.5 and pH 7.4, as shown in Figure S6 and Figure S7 in the Supporting Information. However, for PDP-3 micelles, the CMC values at pH 5.5 and pH 7.4 were quite different because of the disassembly and re-assembly of the crosslinked micelles.

The hydrodynamic radii (R_h) of the amphiphilic aggregates were also measured by DLS, as listed in Table 1 and Figure 2A. At pH 7.4, the average hydrodynamic diameters (R_h) of the crosslinked micelles were 56.4 ± 5.7 nm (PDP-1), 44.2 ± 5.3 nm (PDP-2), and 31.1 ± 4.8 nm (PDP-3), respectively, which were much lower than that of uncrosslinked micelles (PDP-0, 59.9 ± 6.2 nm). Crosslinked micelles had smaller particle diameters due to the reaction between dextran and CNPBA. Interestingly, the shell-crosslinked micelles led to a continuous decrease in R_h as the amount of CNPBA (3.7∼17.3%) increased. The pH-responsive behavior of the micelles was also investigated at different pH values using DLS measurements. As shown in Figure 2B, the R_h of PDP-2 was smaller and the distribution was relatively narrower at pH 7.4. However, there appeared to be a clear bimodal distribution due to the disassembly and re-assembly of PDP-2 micelles in the acidic environment (pH 5.5). The same results could also be certified by transmission electron microscopy (TEM, Figure 2C and 2D). The smaller values from TEM observations when compared to DLS will be due to the dehydration of the micelles in the process of TEM sample preparation. These behaviors can be explained by the fact that the boronate ester bond is unstable and would hydrolyze in an acid environment, resulting in the disassembly and re-assembly of the micelles. All of these findings inferred that the crosslinked micelles had a good response to low pH values.

3.3. In Vitro DOX Loading and Triggered Release

Doxorubicin is a widely used antineoplastic agent in the treatment of several adult and pediatric cancers, which interacts with DNA through insertion and then inhibits the biosynthesis of bioactive macromolecules. In the current study, DOX was used as a model drug and loaded into the micelles. As shown in Table 1, the DLC of PDP-0∼3 were in the range 8.7–10.2% and the DLE were in the range 51.2–61.3%. The data indicated that the stronger crosslinked interaction of the micelles enhanced the drug loading

Macromolecular Journals

Macromol. Biosci. **2014,** DOI: 10.1002/mabi.201400251

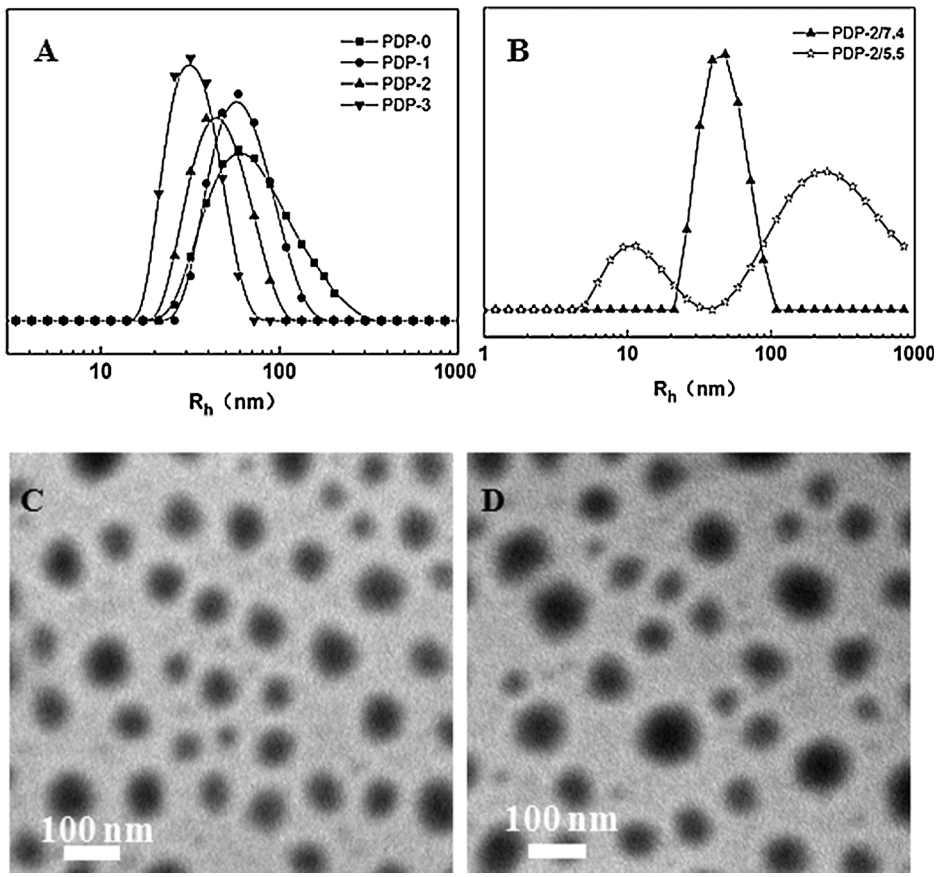

Figure 2. The R_h and size distributions of PDP-m at pH 7.4 (A); the R_h and size distributions of PDP-2 at pH 7.4 and 5.5, respectively (B); TEM micrographs of PDP-2 in pH 7.4 (C) and pH 5.5 (D).

capacity (DLC and DLE). The in vitro release behaviors were investigated at pH 5.3, 6.8, and 7.4. Figure 3 shows the cumulative release percentages of DOX-loaded micelles versus time. From this, it can be concluded that: (1) at the same pH value, a higher ratio of CNPBA in the polymer resulted in a faster release rate and a greater total amount of release, because the boronate ester could improve the hydrophilicity of CNPBA functionalized polymers which resulted in the swelling of the matrix and the release of the payloads; (2) up to 90% of DOX was released from DOX-loaded PDP-3 micelles during the first 12 h in PBS at pH 5.5, and the DOX release rate decreased with increasing pH values 5.5 to 7.4. All this data shows that the DOX-loaded crosslinked micelles have an excellent pH-responsive property and great potential as in vivo intelligent drug delivery vectors.

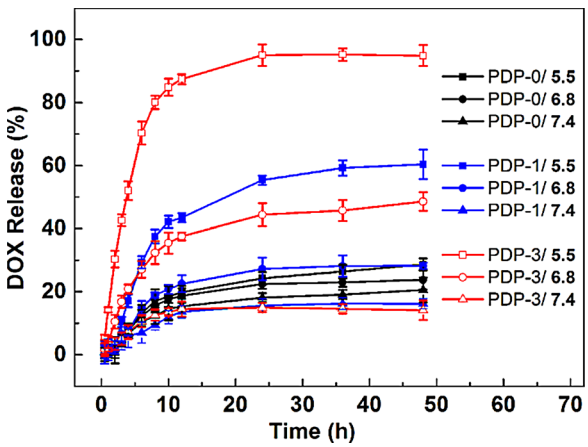

Figure 3. In vitro DOX release from DOX-loaded PDP-m in PBS at pH 5.5, 6.8, and 7.4, respectively.

3.4. Intracellular DOX Release and Cellular Proliferation Inhibition

The cellular uptake and intracellular release behaviors of DOX-loaded micelles were followed with CLSM and flow cytometry toward MCF-7 cells. As expected, a stronger intracellular DOX fluorescence was observed in the cells after incubation with DOX-loaded PDP-3 micelles for 2 h, in contrast to those incubated with DOX-loaded PDP-0 micelle (Figure 4A∼B). The intracellular triggered drug release behavior was further confirmed by flow cytometric analysis. As shown in Figure 5, the flow cytometric

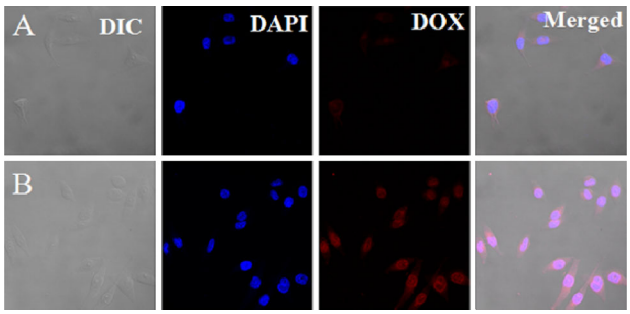

Figure 4. Representative CLSM images of MCF-7 cells incubated with DOX-loaded PDP-0 (A) and DOX-loaded PDP-3 (B). For each panel, the images from left to right show differential interference contrast (DIC) images, cell nuclei stained by DAPI (blue), DOX fluorescence in cells (red), and overlays of the three images.

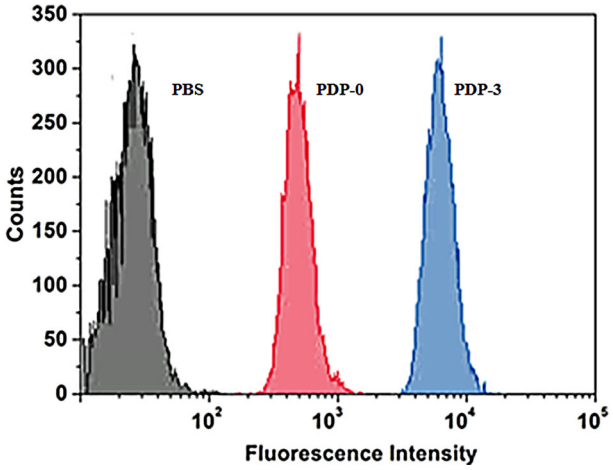

Figure 5. Flow cytometric profiles of MCF-7 cells incubated with PBS, DOX-loaded PDP-0 (a), and DOX-loaded PDP-3 (b) for 2 h.

histogram for the cells incubated with DOX-loaded PDP-3 micelles shifted clearly to the direction of higher fluorescence intensity when compared with the cells incubated with DOX-loaded PDP-0 micelles. This enhanced fluorescence intensity in the MCF-7 cells incubated with DOX-loaded PDP-3 micelles should attributed to the lower pH environment, which induced the swelling of the matrix and the release of the payloads.

It is necessary to evaluate the potential toxicity of polymeric materials for drug delivery applications. Usually MTT, WST-1, and Cell Titer can be used to evaluate the cytotoxicity of cells. Herein, we chose MTT, the method most frequently used in our laboratory, to study the cytotoxicity. The in vitro cytotoxicity of PDP-m to MCF-7 and HeLa cells was evaluated by a MTT assay. As shown in Figure 6, the viabilities of MCF-7 and HeLa cells treated with PDP-0∼3 for 72 h were over 80% at all test concentrations up to 10.0 g L^{-1}. These results suggested that both uncrosslinked and crosslinked micelles had low cytotoxicity and could be safely used as biocompatible carriers for drug delivery.

The in vitro cellular proliferation inhibitions of DOX-loaded PDP-m against MCF-7 and HeLa cells were also estimated by a MTT assay. In contrast to DOX-loaded PDP-0, DOX-loaded PDP-1∼3 exhibited significantly lower growth inhibition efficiency to MCF-7 and HeLa cells (shown in Figure 7), revealing that the mildly acidic environment of the tumor cells could promote the swelling of the micelles and the release of the loaded drug.

4. Conclusion

In this article, 3-carboxy-5-nitrophenylboronic acid (CNPBA) shell-crosslinked micelles based on amphiphilic Dex-*b*-PLA were designed and used for efficient intracellular

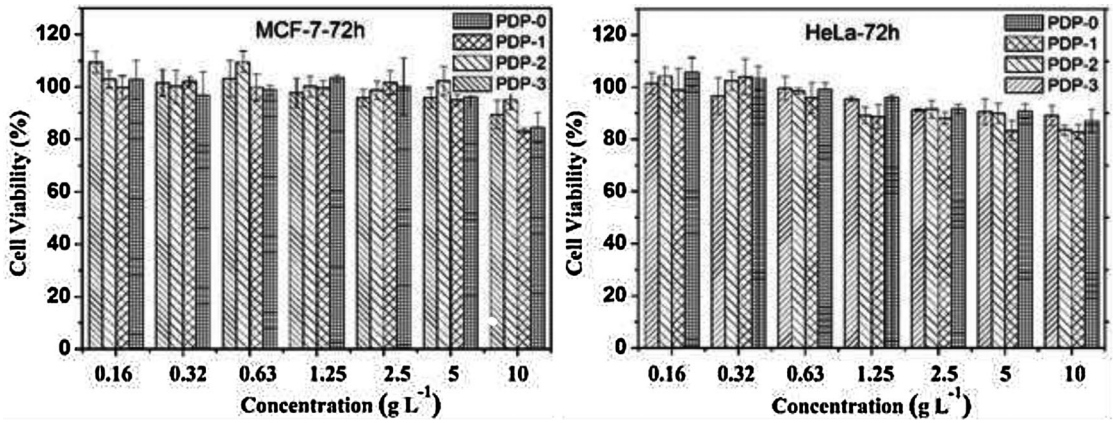

Figure 6. Cytotoxicity of PDP-m towards MCF-7 cells and HeLa cells after incubation for 72 h.

Macromolecular Journals

Macromol. Biosci. **2014,** DOI: 10.1002/mabi.201400251

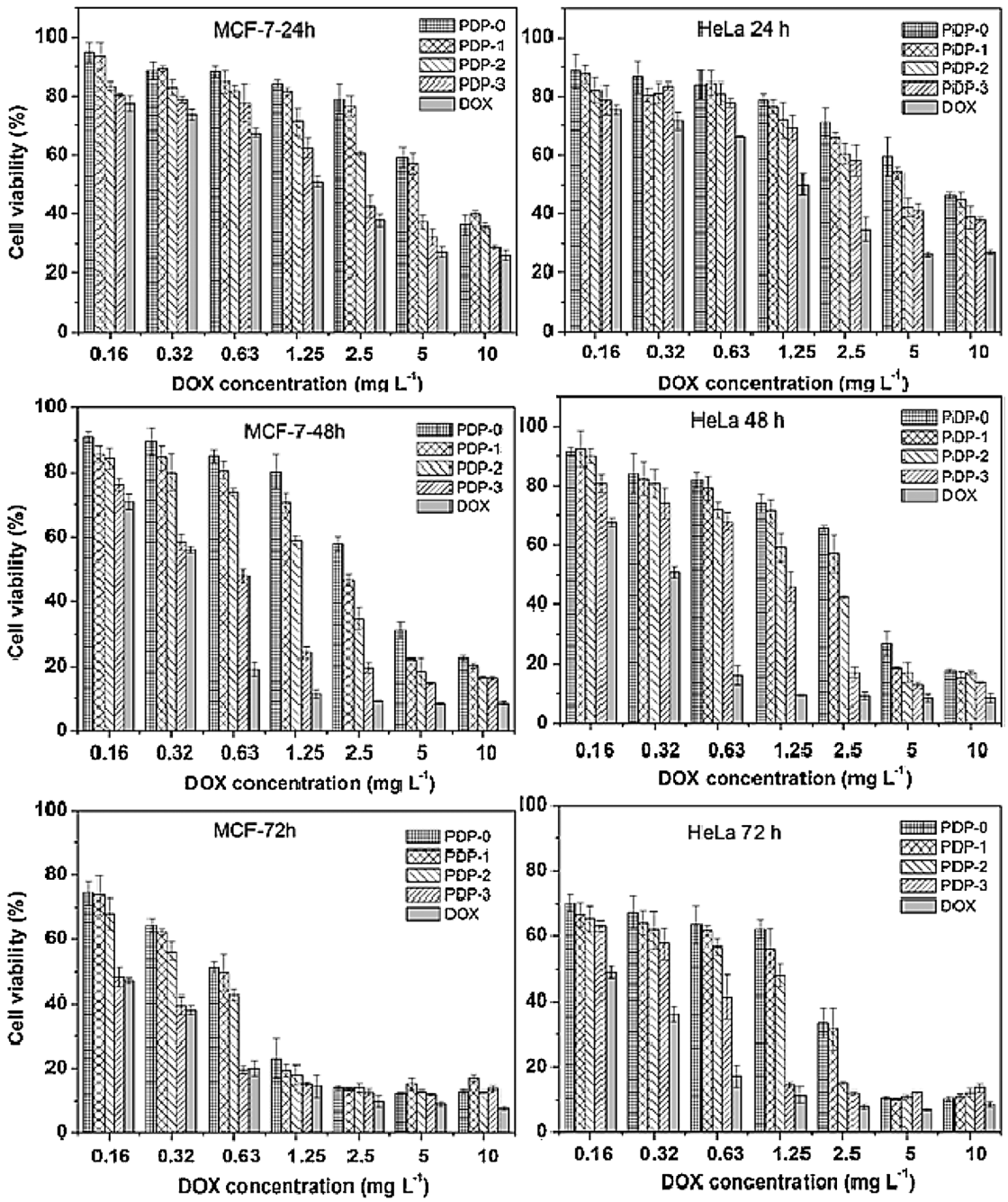

Figure 7. Cytotoxicities of DOX-loaded PDP-m and free DOX toward MCF-7 cells and HeLa cells after incubation for 24 h, 48 h, and 72 h.

drug deliveries. The copolymers were verified by ^{1}H NMR and UV spectra. The CMC, DLS, and TEM data showed that the shell-crosslinked micelles had pH-responsive properties. DOX, as a model anticancer drug, was loaded into PDP-m by a simple dialysis technique. Compared to the uncrosslinked micelles, the crosslinked micelles showed lower CMC values and DOX-loaded crosslinked micelles exhibited a more rapid release rate. The biocompatibilities of micelles and cellular proliferation inhibition of DOX-loaded micelles were also investigated with MCF-7 and HeLa cells. The features identified suggest that these pH-responsive biodegradable nanocarriers can efficiently load and deliver DOX into tumor cells and enhance the inhibition of cellular proliferation in vitro, providing a favorable platform to construct an efficient drug delivery system for cancer therapy.

Supporting Information

Additional characterization data is presented in the Supporting Information, including: ^{1}H NMR spectrum of atactic PLA in $CDCl_3$; ^{1}H NMR spectra of dextran and α-alkyne dextran in DMSO-d_6; FT-IR spectra of PDP-0 and PDP-3; UV-vis standard curve of CNPBA in DMSO; plot of the emission intensity at 660 nm versus the log of concentration (mg mL^{-1}) of PDP-0∼3 micelles at pH 7.4; plot of the emission intensity at 660 nm versus the log of concentration (mg mL^{-1}) of PDP-0 and PDP-3 micelles at pH 5.5 and pH 7.4, respectively.

Acknowledgements: This research was financially supported by the National Natural Science Foundation of China (Projects 51273037, 50903012 and 21174142), Jilin Science and Technology Bureau (20130206074GX, International Cooperation Project 20120729), and Jilin Human Resources and Social Security Bureau (201125020).

Received: May 23, 2014; Revised: July 25, 2014; Published online: DOI: 10.1002/mabi.201400251

Keywords: dextran; drug carriers; micelles; pH-responsiveness; polylactide

[1] X. Chen, L. Chen, X. Yao, Z. Zhang, C. He, J. Zhang, X. Chen, *Chem. Commun.* **2014**, *50*, 3789.
[2] F. Shi, J. Ding, C. Xiao, X. Zhuang, C. He, L. Chen, X. Chen, *J. Mater. Chem.* **2012**, *22*, 14168.
[3] J.-H. Park, H.-J. Cho, H. Y. Yoon, I.-S. Yoon, S.-H. Ko, J.-S. Shim, J.-H. Cho, J. H. Park, K. Kim, I. C. Kwon, *J. Controlled Release* **2014**, *174*, 98.
[4] M. Delcea, H. Möhwald, A. G. Skirtach, *Adv. Drug Delivery Rev.* **2011**, *63*, 730.
[5] Y. K. Joung, J. Y. Jang, J. H. Choi, D. K. Han, K. D. Park, *Molecular Pharmaceutics* **2012**, *10*, 685.
[6] H. Kim, Y. Lee, I. H. Lee, S. Kim, D. Kim, P. E. Saw, J. Lee, M. Choi, Y.-C. Kim, S. Jon, *S. J. Controlled Release* **2014**, *178*, 118.
[7] J. Ding, F. Shi, D. Li, L. Chen, X. Zhuang, X. Chen, *Biomater. Sci.* **2013**, *1*, 633.
[8] S. Deshayes, H. Cabral, T. Ishii, Y. Miura, S. Kobayashi, T. Yamashita, A. Matsumoto, Y. Miyahara, N. Nishiyama, K. Kataoka, *J. Am. Chem. Soc.* **2013**, *135*, 15501.
[9] Y. Li, W. Xiao, K. Xiao, L. Berti, J. Luo, H. P. Tseng, G. Fung, K. S. Lam, *Angew. Chem.* **2012**, *124*, 2918.
[10] L. Jiang, J. W. de Folter, J. Huang, A. P. Philipse, W. K. Kegel, A. V. Petukhov, *Angew. Chem. Int. Ed.* **2013**, *52*, 3364.
[11] B. M. Dicheva, T. Lt. Hagen, L. Li, D. Schipper, A. L. Seynhaeve, G. Cv. Rhoon, A. M. Eggermont, L. H. Lindner, G. A. Koning, *Nano Lett.* **2012**, *13*, 2324.
[12] S. Mathew, T. Murakami, H. Nakatsuji, H. Okamoto, N. Morone, J. E. Heuser, M. Hashida, H. Imahori, *ACS Nano* **2013**, *7*, 8908.
[13] A. G. Skirtach, C. Dejugnat, D. Braun, A. S. Susha, A. L. Rogach, W. J. Parak, H. Möhwald, G. B. Sukhorukov, *Nano Lett.* **2005**, *5*, 1371.
[14] A. Zhang, Z. Zhang, F. Shi, C. Xiao, J. Ding, X. Zhuang, C. He, L. Chen, X. Chen, *Macromol. Biosci.* **2013**, *13*, 1249.
[15] J. Ding, F. Shi, C. Xiao, L. Lin, L. Chen, C. He, X. Zhuang, X. Chen, *Polym. Chem.* **2011**, *2*, 2857.
[16] Y. Wang, K. Zhou, G. Huang, C. Hensley, X. Huang, X. Ma, T. Zhao, B. D. Sumer, R. J. DeBerardinis, J. Gao, *Nat. Mater.* **2014**, *13*, 204.
[17] A. G. Skirtach, A. Muñoz Javier, O. Kreft, K. Köhler, A. Piera Alberola, H. Möhwald, W. J. Parak, G. B. Sukhorukov, *Angew. Chem. Int. Ed.* **2006**, *45*, 4612.
[18] T. Wan, R. Huang, Q. Zhao, L. Xiong, L. Qin, X. Tan, G. Cai, *J. Appl. Polym. Sci.* **2013**, *130*, 3404.
[19] K. Miao, W. Shao, H. Liu, Y. Zhao, *Polym. Chem.* **2014**, *5*, 1191.
[20] O. A. Adegoke, T. E. Adesuji, O. E. Thomas, *Spectrochim. Acta, Part A* **2014**, *128*, 147.
[21] L. Li, Y. Xu, I. Milligan, L. Fu, E. A. Franckowiak, W. Du, *Angew. Chem. Int. Ed.* **2013**, *52*, 13699.
[22] W. Yang, X. Gao, G. Springsteen, B. Wang, *Tetrahedron Lett.* **2002**, *43*, 6339.
[23] D. Roy, J. N. Cambre, B. S. Sumerlin, *Chem. Commun.* **2008**, *21*, 2477.
[24] L. Zhu, S. H. Shabbir, M. Gray, V. M. Lynch, S. Sorey, E. V. Anslyn, *J. Am. Chem. Soc.* **2006**, *128*, 1222.
[25] L. Zhao, J. Ding, C. Xiao, P. He, Z. Tang, X. Pang, X. Zhuang, X. Chen, *J. Mater. Chem.* **2012**, *22*, 12319.
[26] Y. Wen, J. K. Oh, *RSC Advances* **2014**, *4*, 229.
[27] T. Jiang, Z. Zhang, Y. Zhang, H. Lv, J. Zhou, C. Li, L. Hou, Q. Zhang, *Biomaterials* **2012**, *33*, 9246.
[28] W. Scarano, H. T. Duong, H. Lu, P. L. De Souza, M. H. Stenzel, *Biomacromolecules* **2013**, *14*, 962.
[29] Y.-J. Huang, W.-J. Ouyang, X. Wu, Z. Li, J. S. Fossey, T. D. James, Y.-B. Jiang, *J. Am. Chem. Soc.* **2013**, *135*, 1700.
[30] Q. Guo, Z. Wu, X. Zhang, L. Sun, C. Li, *Soft Matter* **2014**, *10*, 911.
[31] R. Ma, L. Shi, *Polym. Chem.* **2014**, *5*, 1503.
[32] Y. Wang, X. Zhang, J. Mu, C. Li, *New J. Chem.* **2013**, *37*, 796.
[33] L. Zhang, Y. Lin, J. Wang, W. Yao, W. Wu, X. Jiang, *Macromol. Rapid Commun.* **2011**, *32*, 534.
[34] L. Li, Z. Bai, P. A. Levkin, *Biomaterials* **2013**, *34*, 8504.
[35] Z. Zhao, Z. Zhang, L. Chen, Y. Cao, C. He, X. Chen, *Langmuir* **2013**, *29*, 13072.
[36] J. L. Mynar, A. P. Goodwin, J. A. Cohen, Y. Ma, G. R. Fleming, J. M. Fréchet, *Chem. Commun.* **2007**, *20*, 2081.
[37] C. Chen, G. Liu, X. Liu, S. Pang, C. Zhu, L. Lv, J. Ji, *Polym. Chem.* **2011**, *2*, 1389.